



**Final report of**

**Network of Research Infrastructures for European Seismology  
NERIES**

Subproject JRA2 "Real time hazard tools"  
Task A "The living Euro-Med earthquake hazard"

**Hybrid zoneless probabilistic  
seismic hazard assessment:  
Test and first application  
to Europe and the Mediterranean**

Chung-Han Chan, Gottfried Grünthal

*GFZ German Research Centre for Geosciences, Potsdam  
Section 2.6 Seismic Hazard and Stress Field, Germany*

## 1. Introduction

The development of new approaches to short-term time-dependent earthquake hazard assessment, i.e. basically probabilistic aftershock forecasting, in the Euro-Mediterranean region on the basis of a E-Science infrastructure is the focus of the NERIES Joint Research Activity JRA2 ([www.neries-eu.org](http://www.neries-eu.org)). Short-term hazard can exceed the hazard from the stationary background in certain locations for periods of days to decades by orders of magnitude (like "24-Hour Aftershock Forecast Map" sometimes also called "The earthquake weather", see also <http://earthquake.usgs.gov/earthquakes/step/>). Also the "background" seismic hazard is, in its closer view, time-dependent in the sense of a "living" Euro-Med earthquake hazard, especially when updated as new significant data becomes available. Then adjustments need to be made. Particularly when detectable changes in seismicity distribution have occurred that significantly alter the hazard. The NERIES task, the generation of the "background" seismic hazard model, which allows easily to be updated, is subject of this paper. Such a 'living' Euro-Med earthquake hazard requires the development of a robust technique and solutions to re-compute hazard automatically when the conditions, as described above, have changed.

Seismic hazard has traditionally been assessed at a national level in Europe. In 1999, a first unified probabilistic seismic hazard assessment (PSHA) for Europe and the Mediterranean (Euro-Med) was published in the framework of GSHAP, i.e. the Global Seismic Hazard Assessment Program (*Grünthal et al.*, 1999a, b). It has been further completed in 2003 for Europe as a whole in the framework of the SESAME, i.e. Seismotectonic and Seismic Hazard Assessment of the Mediterranean Basin (*Jiménez et al.*, 2003).

The living Euro-Med earthquake hazard will of course make use of the most updated seismicity data files and ground motion prediction equations (GMPE). New and improved seismic source zone models could have been provided for a few countries only but not for the entire Euro-Med region. On the other hand, a seismic source zone model always represent a certain view of one group of experts and may subject of changes in future, which hardly can be automated. Therefore, we opted to use a zoneless approach to be as much as flexible with respect to the spatiality of seismicity.

The two basic zoneless approaches are those by *Frankel* (1995) and *Woo* (1996). Both infer the structured character of the seismicity activity density from the recorded or observed earthquakes by a statistical Kernel technique and a magnitude dependent completeness of the seismicity for a certain study area.

Standard model requirement of a zone-based PSHA, such as geometry of seismic source zones and the upper bound or maximum expected magnitude are not required for the zoneless PSHA for non-stationary behavior of seismicity for future automatic applications in cases when the spatial and temporal seismicity

pattern is changing. But large regions like the Euro-Med area are characterized by rather different seismic regimes and regionally varying catalogue completeness.

Thus, for considering spatial differences in both seismicity and catalogue completeness, a new methodology was developed. It is based primarily on the zoneless approach to avoid defining detailed seismic source zones. For its application to large tectonically inhomogeneous regions with strongly different catalogue completeness times and Kernel functions, the introduction of large-scale zones solely based on the large-scale geological architecture and the areal coverage of seismic catalogues is unavoidable.

Accordingly, this approach is called hybrid zoneless approach. In order to test its feasibility, we first apply it to a test area covering southwestern Germany and the adjacent areas of Austria, France, and Switzerland, where (1) considerable PSHA experience exists from previous studies, (2) several tectonic environments join and (3) different national earthquake catalogues with rather different completeness pattern have to be considered. The new approach is further applied to the entire Euro-Med region, which is characterized by different GMPEs for different parts of the study area, which can also easily be associated with single large-scale zones.

## 2. Seismicity and tectonic setting

### 2.1. The seismicity data file and its declustering

The seismicity data file used for this study is represented by the earthquake catalogue CENEC for Europe north of 44°N (*Grünthal et al.*, 2009a). This paper describes in detail how this homogeneous data file in terms of moment magnitudes  $M_w$  (with  $M_w \geq 3.5$ ) has been derived. The degree of harmonization achieved in CENEC is quantitatively analyzed in *Grünthal et al.* (2009b). The extension of CENEC to the south in connection with an update of CENEC is represented by the Euro-Mediterranean earthquake catalogue EMEC, which is briefly described in *Grünthal & Wahlström* (2009). CENEC stands for CEntral, Northern and northwestern European earthquake Catalogue and EMEC for Euro-Mediterranean Earthquake Catalogue. This earthquake catalogue incorporates about 60 local catalogues and 80 special studies of earthquakes in central, northern, northwestern and southern Europe, northwestern Africa, and Turkey.

EMEC follows the same principles as described for CENEC. The lower threshold magnitude in the southern part of EMEC; i.e. south of the CENEC area, varies between  $M_w \geq 3.5$  to  $M_w \geq 4.5$ . A corresponding paper which describes the catalogue works in detail with the reference to the publicly available seismicity data file is under way. We make use of the stage of the project for preparing the har-

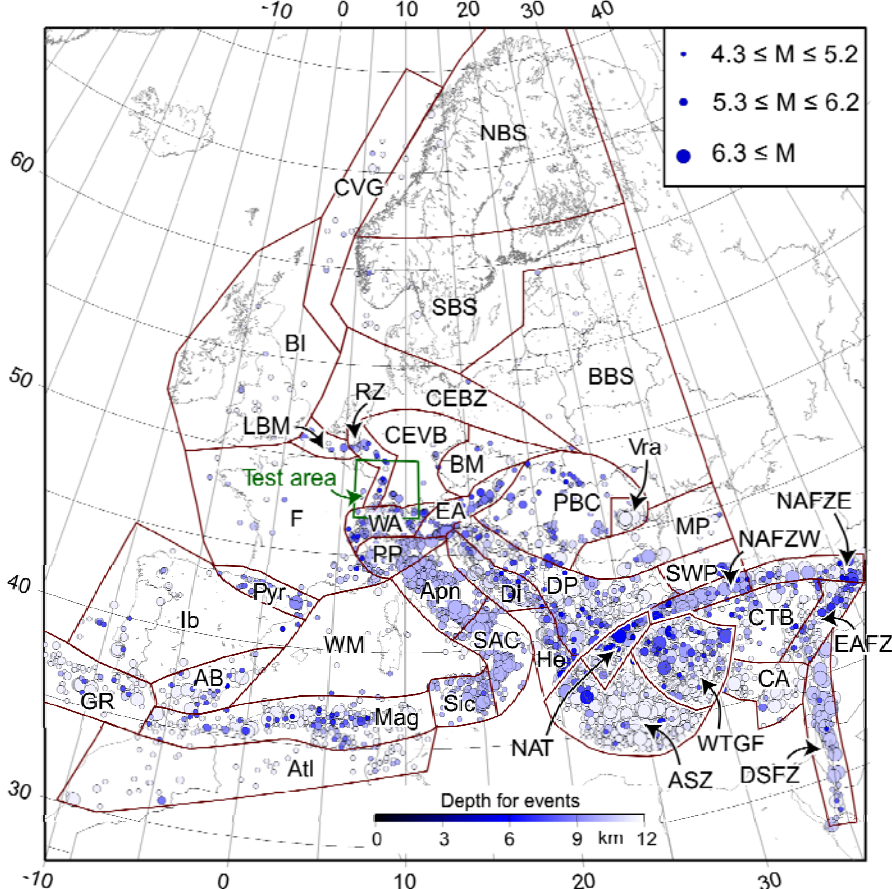


**Figure 1.** Distribution of seismicity and large-scale zones in the entire study area. Dark blue circles represent shallow earthquakes, light blue circles represent deep earthquakes; large circles represent earthquakes with higher magnitude, small circles represent earthquakes with lower magnitude. The zone marked by green lines is test area for the hybrid approach and is shown in detail in Fig. 2.

monized seismicity data file as per March 2010. The earthquakes, with a harmonized  $M_w$  for the Euro-Med region sensu lato are shown in Figure 1.

Due to the limitations in the ground motion models (cf. chapter 3) the PSHA is restricted to earthquakes with  $M_w \geq 4.3$ . Areas of increased seismic activity can clearly be identified in Figure 1. These are the southern parts of the Balkans, western Turkey, Italy, the Alpine area, SE Iberia and the Maghreb region in NW Africa.

The seismicity data pre-processing consists of two steps: Firstly, the declustering, i.e. the removal of foreshocks and aftershocks, and secondly, the analysis of data completeness with time (described in chapter 4).

The declustering applied here follows the robust and rigorous method by Grünthal (1985), which was extended to larger magnitudes (Burkhard & Grünthal, 2009; Grünthal *et al.*, 2009a). Although originally developed for central European conditions, it proved equally applicable for a study for the Levant (Grünthal *et al.*, 2009b) and even for a subduction environment (Suckale & Grünthal, 2009). It will be used here as well.

## 2.2. Tectonic setting and zonation

We introduced a large-scale zone model (LSZM) (Figure 1) in order to derive a reliable seismicity density rate, which considers spatial differences in seismicity data completeness. At the same time the LSZM should also accommodate differences in spatial seismicity density (which is related to the bandwidth function described in chapter 4) and the possibility to introduce different ground motion models in such large-scale zones. The basic principle in defining the LSZM consists in delineating a model, which reflects the large-scale geological and tectonic architecture. The NERIES JRA2 study area covers regionally Europe and the Mediterranean area except eastern Europe and the southeastern part of the Mediterranean off-shore and on-shore areas (Figure 1). Tectonically, this region represents the western part of the Eurasian plate up to its continental shelf as well as the seismic active plate boundary areas to the south including the microplates north of the Aegean and the Cyprian arc.

The large scale zones (LSZ), as they are shown in Figure 1, mirror first of all the active plate boundary between the Eurasian and the African plate with the Apulian promontory acting as an indenter of African crust towards the north. The plate boundary related LSZ (from west to east) are the Gibraltar rift (GR), the Maghreb (Mag), and the seismically active Atlas mountains (Atl), Sicily (Sic), the southern Apennines and Calabria (SAC), the Apennines (Apn), and the Po plain with adjacent mountain areas (PP). The subdivision of Italy into four sub-regions with respect to catalogue completeness characteristics follow basically *Stucci et al.* (2004). North of the Apulian promontory the Alps have been upfolded, which are separated into the western Alps (WA) and the eastern Alps (EA). Both areas have significantly different seismicity characteristics. The eastern shoulder of the Apulian promontory is represented by the Dinarides (Di), and the Hellenides (He). Further south, the plate boundary merges into the Aegean subduction zone (ASZ), North Aegean troughs (NAT), the W-Turkish graben formations (WTGF), and continues into the North Anatolian fault zone west (NAFZW) and the North Anatolian fault zone east (NAFZE). The microplate of the central Turkish block (CTB) is bounded to the south and east by the Cyprian arc (CA) and the East Anatolian fault zone (EAFZ). Included into the study area is also the adjoining Dead Sea fault zone (DSFZ).

The northeast of the study area is built up by the Baltic shield (separated due to different seismicity characteristics in a northern and southern part NBS and SBS) and the Baltic Belarus syncline (BBS) as part of the east European platform. Tectonically and with respect to the seismicity more active units (or LSZ) of the Variscian W-European crust are the Rhine graben zone (RZ), the central and the Viking (CVG) graben in the North Sea, the London Brabant massif (LBM), the Pyrenees (Pyr), and the Alboran block (AB) in SE Spain. The remaining areas of western

Europe with lower tectonic and seismic activity are those covering the rest of the Iberian peninsula (Ib), France (F), and British islands and Ireland (BI).

The Alpidic area NE of the Apulian promontory is built by the Pannonian Basin with the surrounding Carpathian mountain belt (PBC). The south-eastern tip of the PBC is captured by the intermediate depth (with hypocentral depth between 70 and 150 km) high seismicity LSZ of the Vrancea (Vra). Also of Alpidic origin SW of the PBC extend the eastern Dinarides, which continue in southeasterly directions into the Pelagonides and Balkanides (DP), which altogether built one LSZ. Further east are the Moesian plate (MP) and the SW Pontus block (SWP) as two further LSZs.

North of the Alps and NW of the PBC extend the Central European Variscian block (CEVB), the Bohemian massif with the Lugicum (BM) as well as the central European basin zone (CEBZ).

The test area of this study (Figure 2) covers geographically SW Germany with the adjoining parts of France, northern Switzerland and the northwesternmost tip of Austria. According to the subdivision of the area into LSZs, characterizing the large scale tectonic architecture, these are parts of the Rhine graben zone (RZ), the central European Variscian block (CEVB), the western Alps (WA), and the one labeled as France (F).

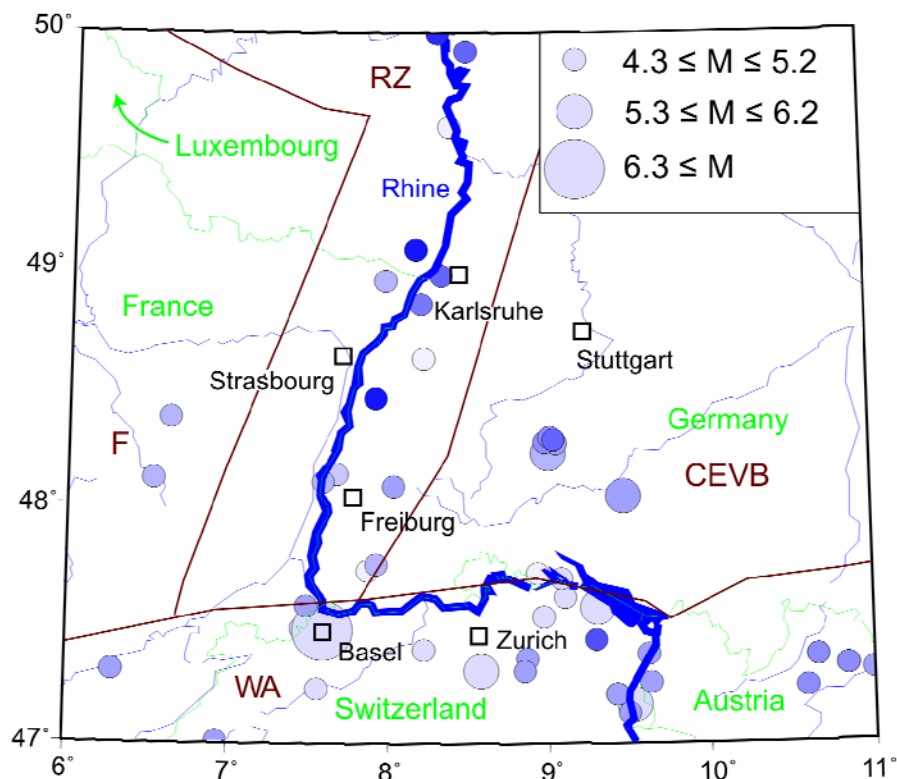


**Figure 2.** Distribution of seismicity and large-scale zone in the test area (marked by green lines in Fig. 1). Dark blue circles represent shallow earthquakes, light blue circles represent deep earthquakes; open circles represent earthquakes with unknown depth; large circles represent earthquakes with higher magnitude, small circles represent earthquakes with lower magnitude. CEVB, F, RZ, and WA denote zone of the Central European basin zone, France, Rhine graben zone, and Western Alps, respectively.

### 3. Ground motion prediction equations

A pan-European PSHA requires for using appropriate ground motion prediction equations (GMPE), to consider the differences in models for shallow- and intermediate depth earthquakes in subduction areas like the Aegean subduction zone (ASZ), North Aegean troughs (NAT), the Cyprus arc (CA), and the Vrancea (Vra).

Since this study does not aim at considering the full epistemic uncertainties usually contained in a PSHA we restrict ourselves to apply one GMPE for crustal earthquakes. Following the recommendations given in *Scherbaum et al.* (2005) for choosing suitable GMPE for a pan-European study, there remains the relationships given by *Ambraseys et al.* (1996) and by *Berge-Thierry et al.* (2003) where the former is superseded by the latter. In a similar analysis for choosing reliable GMPE by *Drouet et al.* (2007) with the focus on the Pyrenees, the only GMPE based on European and Middle East data was that by *Berge-Thierry et al.* (2003).

Other decision criteria for choosing suitable GMPEs to be applied here are (1) the inclusion of focal depth in the GMPE, since the hazard in e.g. central and northern Europe is to a large extent caused by smaller magnitude earthquakes with  $M_w$  in between 4.0 and 5.0, and (2) that the respective GMPE explicitly has been based on such smaller events. These two latter criteria are not fulfilled by two more modern models by *Akkar and Bommer* (2007, 2010), which have been developed also entirely on records from Europe, the Mediterranean region and the Middle East. They do not use the focal depth as a parameter and magnitudes on the range of 5.0 to 7.6. But the *Berge-Thierry et al.* (2003) model does include the focal depth as a parameter and it does include magnitudes in a range starting at  $M = 4.0$ . The usage of both parameters i.e. (1) the focal depth of the events and (2) the magnitudes in a range starting at  $M = 4.0$  is of importance in zoneless PSHA. In contrary, in zone-based approaches the frequency-magnitude parameter can be derived from small magnitude earthquakes (e.g. in the range of  $M = 2.0\text{--}4.0$ ) while the integration procedure in the hazard calculation itself can rely on a minimum magnitude of say 5.0. This is not possible in zoneless PSHA. Here the integration has to be performed for the events in the same magnitude range, where the GMPE is valid. Moreover, the focal depth of each event is considered directly as input in a zoneless approach. All the reasons described above led to the conclusion to make use of the GMPE by *Berge-Thierry et al.* (2003).

This model describes the evolution of the spectral acceleration with respect to the magnitude, the hypocentral distance and the site category. Since the *Berge-Thierry et al.* (2003) GMPE is based on surface wave magnitude  $M_s$  but the exerted seismicity data are harmonized in terms of moment magnitude  $M_w$ , a relation between  $M_s$  and  $M_w$  has to be applied. As appropriate conversion relation is

used the one by *Bungum et al.* (2003), which yields for northern Europe  $M_S = M_w$  while for southern Europe (Latitude  $\leq 47.5^\circ$ ) the derived relation reads:

$$M_S = -7.176 + 3.062M_w - 0.148M_w^2 \quad \text{for } M_S \leq 6.5;$$

$$M_S = M_w \quad \text{for } M_S > 6.5.$$

Due to special attenuation characters for the intermediate depth events (depth  $\geq 70$  km) in the Vrancea region, Romania, consideration of another GMPE is required. Because strong motion records for Vrancea events are scarce, most of GMPE are based on macroseismic data (*Ivan et al.*, 1998; *Mandrescu and Radulian*, 1999; *Mandrescu et al.*, 1988) and describe the intensity attenuation. To apply these models for our purpose, it is necessary to introduce a relation between intensity and peak ground acceleration (PGA) or spectral acceleration (PSA). Such relations, however, are scarce as well. Thus, we consider the ground motion model for PGA and PSA by *Sokolov et al.* (2008). This model is acquired from regression of four of the large ( $M_w \geq 6.3$ ) since 1977 and some small to moderate ( $M_w < 6.3$ ) earthquakes during 1990 and 2002. Using this model site amplification terms for each seismic source zone are necessary. For our hybrid zoneless PSHA site amplification factor as by *Borcherdt* (1994) are used.

The other region, where a specific GMPE is needed, is the Hellenic Arc system. Since all of GMPEs for this region consider macroseismic data (e.g. *Papazachos et al.*, 1993; *Papaioannou and Papazachos*, 2000), the GMPE for global subduction earthquakes by *Atkinson and Boore* (2003) is thus considered in this study. In order to simplify the calculation, we only consider the ground motion model for in-slab earthquakes.

## 4. Methodology

### 4.1. Standard zoneless approach

The standard procedure of the traditional PSHA (*Cornell*, 1968) is based on the estimation of the mean number of annual exceedances  $\nu(z)$  of an expected ground motion level  $z$  at the assessed sites, which can be expressed as:

$$\nu(z) = \sum_{i,j} \lambda(M_i)P(r_j|M_i)G(z|M_i, r_j)$$

where  $\lambda(M_i)$  represents the mean number of earthquakes per time unit as a function of magnitude  $M_i$ ,  $P(r_j|M_i)$  represents the probability of an earthquake of magnitude  $M_i$  at a distance  $r_j$  from the site, and  $G(z|M_i, r_j)$  is the probability that the

ground motion level will be exceeded, given an earthquake of magnitude  $M_i$  at a distance  $r_j$  from the assessed site.

For the standard zoneless approach, we introduce the density of seismic activity rate inferred from past earthquakes. *Riznichenko* (1965) first proposed the estimation of seismic hazard by shakability that represents the areal distribution of the mean seismicity rate in the seismic catalogue which later was extended towards a kind of a zoneless approach. *Frankel* (1995) used the Gaussian distribution as smoothing operation for estimation of seismicity rate representing the seismic density decay with distance from the epicenters of past events. For the approach developed by *Woo* (1996), the Kernel function  $K(M, r)$  as a function of magnitude  $M_i$  and hypocentral distance  $r_j$  is introduced as a smoothing operation to represent the probability distribution of earthquakes:

$$K(M_i, r_j) = \frac{PL-1}{\pi H^2(M_i)} \left(1 + \left(\frac{r_j}{H(M_i)}\right)^2\right)^{-PL},$$

where  $PL$  denotes the power law index. Recommended  $PL$  values are between 1.5 and 2.0, which corresponds to a cubic or quadratic decay with hypocentral distance  $r_j$  (*Molina et al.*, 2001). Since we found that the difference of the results is insignificant when  $PL$  is assumed to be in between 1.5 and 2, we assume  $PL = 2.0$  in this study.  $H(M)$  is a bandwidth function represented as  $H(M) = c \cdot e^{d \cdot M}$ , which suggests that the distance between two events is an exponential function of magnitude. Since the Kernel function considers not only density decay with distance, but also the magnitude of the earthquake, we apply *Woo's* approach for PSHA and improve its capabilities by further revisions.

For the standard zoneless approach, the seismicity is not required to be Poissonian. In order to compare our results with those on the zone-based approach, however, the declustering is introduced to eliminate foreshocks and aftershocks from the earthquake catalogue (cf. chapter 2). In the following we apply the standard zoneless approach to SW Germany with its adjacent region (Figure 2) to compare it with PSHA results obtained by a zone-based study and to test its feasibility, by introducing the innovations one after the other.

As it has been already said, the study area has been separated into four large-scale zones according to the large-scale geological architecture. Those are the Central European Variscian block (CEVB), France (F), Rhine graben zone (RZ), and western Alps (WA) (cf. chapter 2). A higher seismicity rate is observed along RZ, in northern Switzerland, and in a cluster ca. 50 km SSW of Stuttgart, i.e. in the area of Albstadt. Earthquakes with focal depths larger than 12 km are mainly observed in NW Switzerland as well as in CEVB. Some of the events along the RZ, by contrast, are shallower (depth of 2 km). The average focal depth of the seismicity in NW Switzerland is about 10 km, that is 1 km more than in the entire test area.

Since the standard zoneless approach cannot consider different completeness, we use for testing the one of the zone CEVB (Table 1). Compared with other large-scale zones in the test area (i.e. F, RZ, and WA), the catalogue completeness times for the CEVB are longer. The bandwidth function with the 95% confidence intervals for the entire test area is shown in Figure 3a. The distribution of focal depths is acquired from the earthquakes in the test area (Table 2). In this study, earthquakes with  $M_w \geq 4.3$  are considered for the seismic hazard assessment.

**Table 1.** The completeness time of each magnitude bin for each large-scale zone.

Name	Magnitude												
	3,5	4	4,5	5	5,5	6	6,5	7	7,5	8	8,5	9	9,5
<b>AB</b>	1970	1950	1950	1950	1950	1820	1750	1650	1350	1350	1350		
<b>Apn</b>	2002	2000	1950	1875	1780	1400	1400	1000					
<b>ASZ</b>	1963	1963	1963	1910	1910	1700	1500	1500	400	400	400	400	
<b>Atl</b>	1960	1950	1950	1920	1920	1870	1700	1700	1700				
<b>BBS</b>	1955	1890	1890	1850	1800	1800							
<b>BI</b>	1970	1875	1865	1840									
<b>BM</b>	1900	1810	1810	1870	1500	1400	1000						
<b>CA</b>	1987	1983	1964	1920	1900	1900	1000	800	800	800	800		
<b>CEBZ</b>	1850	1675	1500	1300	1300	1300							
<b>CEVB</b>	1925	1875	1870	1820	1600	1000	1000	1250					
<b>CTB</b>	2000	1995	1963	1950	1900	1900	1800	1800	1800	1200			
<b>CVG</b>	1981	1955	1950	1900	1860	1850							
<b>Di</b>	1900	1900	1900	1840	1840	1840	1280	1280					
<b>DP</b>	1900	1900	1900	1840	1840	1840	1280	1280					
<b>DSFZ</b>	1985	1960	1960	1920	1890	1720	450	-75	-525				
<b>EA</b>	1895	1850	1800	1760	1550	1400	1400						
<b>EAFZ</b>	2000	1995	1963	1950	1900	1900	1800	1800	1800	1200			
<b>F</b>	1930	1925	1925	1800	1650								
<b>GR</b>	1970	1950	1950	1950	1950	1820	1750	1650	1350	1350	1350		
<b>He</b>		1980	1970	1963	1920	1855	1830	1700					
<b>Ib</b>	1970	1950	1950	1950	1950	1820	1750	1650	1350	1350	1350		
<b>LBM</b>	1925	1890	1860	1860	1300	1300							
<b>Mag</b>	1960	1950	1950	1920	1920	1870	1700	1700	1700				
<b>MP</b>	1930	1900	1900	1900	1900	1800	1700	1700					
<b>NAFZE</b>	2000	1995	1963	1950	1900	1900	1800	1800	1800	1200			
<b>NAFZW</b>	1975	1975	1970	1960	1900	1900	1600	1600	1200	1200			
<b>NAT</b>		1963	1963	1963	1910	1910	1700	1500	1500	400	400	400	400
<b>NBS</b>	1963	1880	1880	1800	1800	1800							
<b>PBC</b>	1860	1840	1800	1800	1700	1700							
<b>PP</b>	2000	2000	1900	1875	1780	1400	1400	1000					
<b>Pyr</b>	1970	1920	1860	1850	1850	1350	1350						
<b>RZ</b>	1925	1875	1870	1820	1600	1000	1000	1250					
<b>SAC</b>	2002	2002	1900	1840	1820	1750	1550	1550					
<b>SBS</b>	1970	1880	1880	1800	1700								
<b>Sic</b>	2002	2002	1960	1910	1910	1750	350	350					
<b>SWP</b>	1975	1975	1970	1960	1900	1900	1600	1600	1200	1200			
<b>Vra</b>			1990	1950	1925	1900	1775	1500	1100				
<b>WA</b>	1880	1860	1825	1770	1650	1575	1250	1250					
<b>WM</b>			1975	1900	1900	1900							
<b>WTGF</b>	1975	1975	1970	1960	1900	1900	1600	1600	1200	1200			

The resulting hazard in terms of PGA with a 10% probability of exceedence in 50 years is shown in Figure 4a. Since the probability density of earthquake occurrence is evaluated according to a smoothing Kernel based on previous events, it suggests a higher seismic hazard where earthquakes occurred more frequently in the past. The highest hazard,  $\text{PGA} = 1.55 \text{ m/s}^2$  is predicted in the region of Albstadt. The other area of increased seismic hazard ( $\text{PGA } 1.0 \text{ m/s}^2$ ) is represen-

ted by the area of Basel at the southern boundary of the Rhine graben zone (RZ).

#### *4.2. The hybrid zoneless approach*

Due to the limitation of the standard zoneless approaches, such as distribution scheme of depth, unalterable catalogue completeness time, unified bandwidth function, and fixed ground motion model for the entire hazard assessed area, it can hardly be applied to large regions like entire Europe. Thus, we developed a new version of the zoneless approach, which consists of the following characteristics:

1. use of the basic elements of the standard zoneless approach developed by Woo (1996);
2. considering the actual depth of each earthquake;
3. introduction of large-scale zones based mainly on the large-scale geological architecture (rather than seismicity pattern) in order to accommodate:
  - varying completeness times; i.e. one fixed completeness model for each of the large-scale zones;
  - varying bandwidth functions; i.e. one fixed bandwidth function for each of the large-scale zones.
  - varying ground motion models (GMPE); i.e. one (or more) fixed GMPEs for each of the large scale zones.

Since this new methodology is based on a standard zoneless approach and further modified by introducing a large-scale zonation, we denote it as 'hybrid zoneless approach'.

When the standard zoneless approach is applied, the depth is introduced through a distribution scheme as shown in Table 2. This simplifying concept, however, can be improved and which has been realized for the hybrid zoneless approach, in such a way that the actual depth of each earthquake is considered separately. The resulting hazard map represented this innovation is shown in Figure 4b.

**Table 2.** The weighting of hypocentral depth in the test area used by the standard zoneless approach (Woo, 1996).

Depth (km)	2	3	5	6
Weighting	6%	8%	9%	11%
Depth (km)	7	8	10	12
Weighting	10%	14%	14%	27%

The comparison with the results obtained without this innovation according to the standard approach is given in Figure 4e. The systematic deviations in depths,

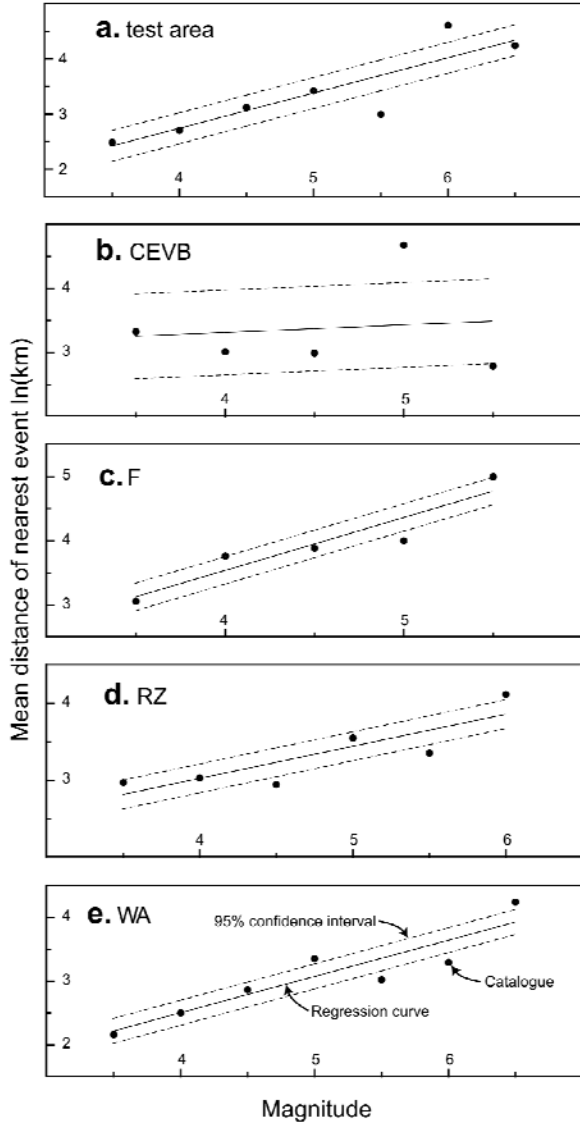


**Figure 3.** Bandwidth functions and 95% confidence intervals for (a) entire test region; (b) zone CEVB (Central European basin zone); (c) F (France); (d) RZ (Rhine graben zone); and (e) WA (Western Alps).

e.g. in the northern Switzerland or in the Rhine Graben zone with lower depths becomes obvious.

Accounting for the differences in the completeness time within each zone (Table 1), the probabilistic hazard is acquired (Figure 4c). The comparison with the results based on a single completeness pattern for the entire test area (Figure 4f), yields PGA being  $0.2 \text{ m/s}^2$  larger in the northern Switzerland and in the western Austria (zone WA). This is due to the more precise estimate of the mean number of earthquakes per unit time as a consequence of using the correct completeness time.

Finally the effect of using different bandwidth functions that represent the density of seismicity for different areas is discussed. By regression of the earthquakes that occurred posterior to the catalogue completeness time in each zone (Table 1), bandwidth functions for each large-scale zone are acquired (see Figure 3b-d). In

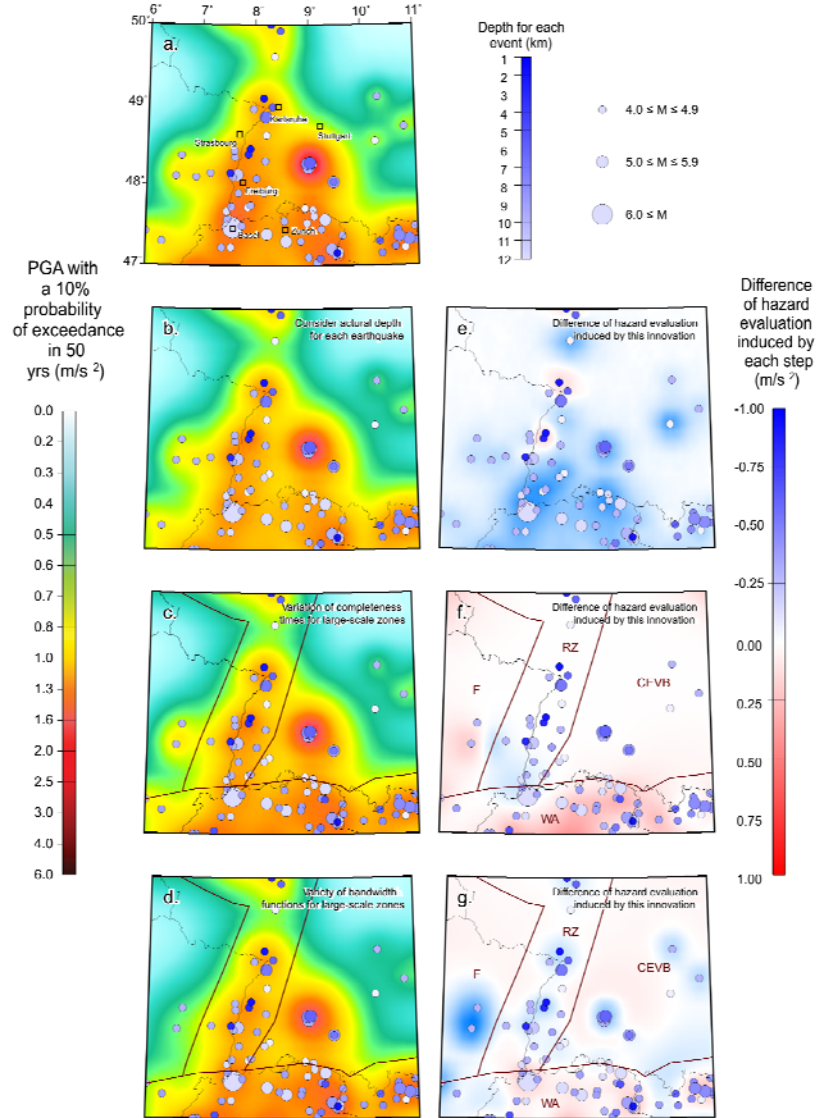


**Figure 4.** The peak ground acceleration (PGA) with a 10% probability of exceedance in 50 years assessed by (a) the standard zoneless approach (Woo, 1996) and each innovation of the hybrid approach, that is (b) to consider actual depth for each earthquake, (c) to consider variation of completeness times for large-scale zones, and (d) to consider variety of bandwidth function for large-scale zones. (e, f, g) represent differences of hazard evaluation induced by the innovations.

comparison with the bandwidth function for the entire test area (Figure 3a), the zones CEVB, F, and RZ show higher level of the bandwidth function; i.e. longer spatial distances between the events. In the zone WA, in contrary, the mean distances between each event is shorter than in the entire test area.

The PSHA, as mentioned, was assessed considering different bandwidth functions (Figure 4d). Comparing this with the results based on a single bandwidth function for the entire test area (Figure 4g), significantly lower hazard levels is acquired. The largest decrease of  $0.27 \text{ m/s}^2$  is observed around the hypocenters of each event in the zone CEVB, F, and RZ, due to the fact that the seismicity is here sparser than the average of in the entire test area. In the zone WA, where seismicity rate is higher (lower level of bandwidth function), a higher level of PGA of

$0.13 \text{ m/s}^2$  is obtained. Figure 4a represents the finally resulting PSHA for the test area, which later will be compared with a hazard map of a zone-based approach.

#### *4.3. Contribution of the bandwidth uncertainty on the hazard results*

We estimate the probabilistic seismic hazard for the test area based on the seismicity rate through a bandwidth function working as a smoothing Kernel in the neighbouring region of earthquakes. The bandwidth function for each large-scale zone is acquired through regression of the earthquake catalogue (Figure 3). In order to check the hazard uncertainty related to this regression, we compare the probabilistic seismic hazard corresponding to the upper and lower bounds of 95% confidence intervals of the bandwidth function in each zone (Figure 5). According to the lower bounds of 95% confidence intervals of the bandwidth function, significant higher hazard is estimated where earthquakes occurred frequently in the past. For Albstadt, 50 km south of Stuttgart, for example, a  $0.9 \text{ m/s}^2$  higher hazard is predicted. In the region where few earthquakes occurred, by contrast, higher hazard is estimated if the upper bound of 95% confidence intervals of the bandwidth function is considered. Besides, larger uncertainties are estimated in the zone CEVB, this phenomenon can be attributed to large deviation of the bandwidth function in this zone (Figure 3b).

#### *4.4. Comparison to standard zone-based approach*

Application of the zone-based approach by Cornell (1968) and McGuire (1976) requires the knowledge of properties of the seismic source zones, such as geometry of each zone, maximum possible magnitudes, Gutenberg-Richter law, and distribution of focal depth. Such information is acquired by some subjective judgments that are usually changes between different studies. In contrast, zonation for the hybrid zoneless approach is based on the variation of earthquake catalogue completeness time and density of seismicity as bandwidth function, and the geometry of large-scale zones for this approach is simply derived from the large-scale geological architecture.

Another requirement parameter for PSHA is the maximum possible magnitude. For the zone-based approach, significantly different hazard levels are obtained when different values of this parameter are assumed. The way of estimating this parameter, however, varies in different studies. In order to test the effect of changing the maximum magnitude on the results of the hybrid zoneless approach, different maximum possible magnitudes, which are 0.5 and 2.0 units higher than the maximum historical magnitudes, are assumed and hazard results for test area are represented in Figure 6. For this approach, the probability of

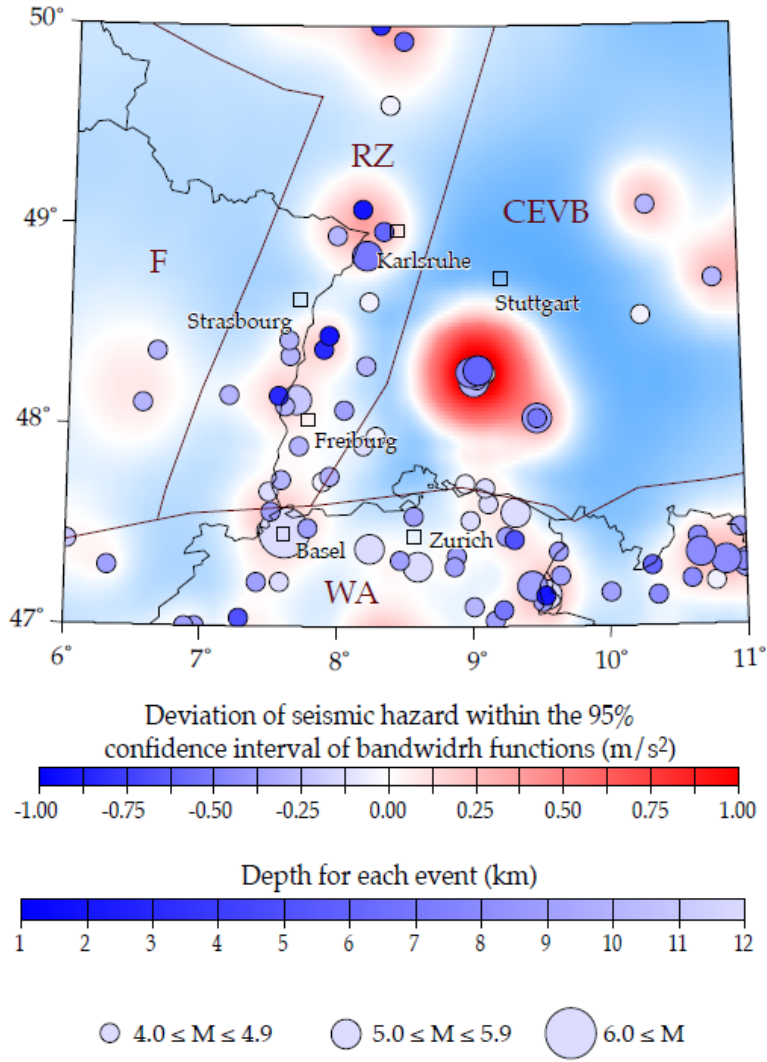


**Figure 5.** The deviation of seismic hazard (the peak ground acceleration with a 10% probability of exceedence in 50 years) between upper and lower boundary of the 95% confidence interval of bandwidth functions.

assigning a given target magnitude follows a Gaussian distribution (Figure 6c). It suggests insignificant influence of this parameter for the approach due to the low probability of occurrence for large magnitudes.

When comparing the PSHA results of the zone-based approach by Grünthal *et al.* (2006) and the hybrid zoneless approach (shown in Figure 7), a fairly good agreement with respect to the locations of peak hazard is observed, such as at the location of Albstadt, along the Rhine Graben, and in northern Switzerland (Figure 7a). The zone-based approach predicts similar peak hazard levels, but lower levels in areas in between (Figure 7b). A previous study (Beauval *et al.*, 2006) observed a similar phenomenon for France. These rapid decays for the zone-based results may be attributed to demarcations between seismic source zones with significant contrasts of seismic rate.

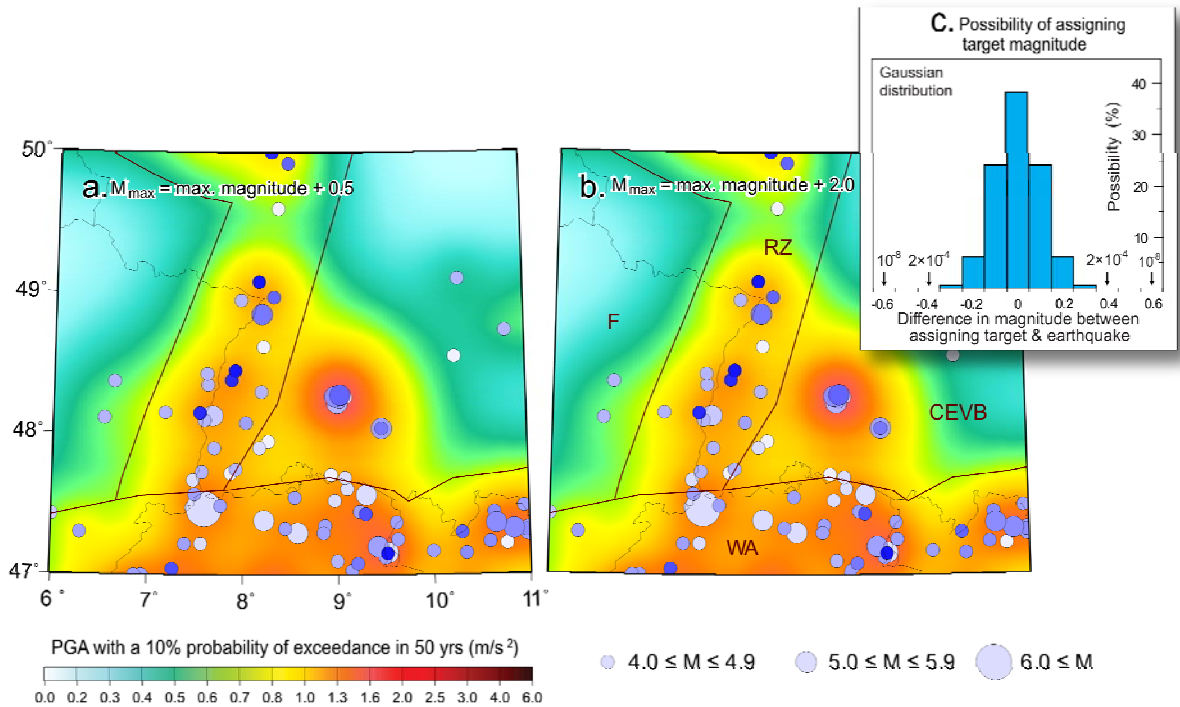


**Figure 6.** Comparison of PSHA results by different maximum possible magnitudes. Maximum possible magnitudes are assumed (a) 0.5 and (b) 2.0 units higher than maximum historical magnitudes. (c) For hybrid zoneless approach, the possibility of assessing target magnitude keeps Gaussian distribution with the difference from earthquake magnitude.

## 5. Probabilistic seismic hazard assessment for the Euro-Med region

In the previous chapters, we have represented the distribution of seismicity (Figure 1), spatial distribution of large-scale zones (Figure 1), the completeness time (Table 1) and bandwidth function (Table 3) within each zone, and the ground motion models for the Euro-Med region. By considering this information, we evaluate the Euro-Med probabilistic seismic hazard map (PGA with 10% probability of exceedence in 50 years) through the hybrid zoneless approach (Figure 8a) and compare it with the GSHAP results (Figure 9b) (Grünthal *et al.*, 1999a, b).

In addition to the standard methodology of using point sources we adopted for selected parts of the study area with earthquake magnitudes of  $M_w \geq 7$  extended sources. This is the case for the North Anatolian fault zone separated into the North Anatolian fault zone west (NAFZW) and its eastern part (NAFZE). Since the ground motion behaviors of large earthquakes cannot truly be represented by point sources, we assume rupture fault geometry for each earthquake. We assume strike = 80° for the earthquakes in NAFZW and 110° in NAFZE, and a dip of 90°. We adopt rupture faults dimensions derived from the scaling laws of Wells and Coppersmith (1994) for a strike-slip focal mechanism:

$$\log(L) = -2.57 + 0.62M_w$$

$$\log(W) = -0.76 + 0.27M_w$$

**Table 3.** Bandwidth function in represented of c- and d-values and average depth in each large-scale zone.

Name	c-value	d-value	Avg. depth
AB	0,449	0,927	29
Apn	15,090	0,150	10
ASZ	3,842	0,328	51
Atl	0,187	1,341	24
BBS	608,300	-0,230	20
BI	14,650	0,359	14
BM	12,420	0,551	13
CA	2,561	0,431	28
CEBZ	39,000	0,000	9
CEVB	16,930	0,118	10
CTB	1,808	0,655	20
CVG	3,753	0,731	21
Di	1,518	0,497	12
DP	1,077	0,644	14
DSFZ	10,310	0,238	11
EA	1,535	0,557	8
EAFZ	3,724	0,409	23
F	1,264	0,822	11
GR	13,010	0,171	32
He	6,717	0,213	21
Ib	8,979	0,449	15
LBM	5,433	0,497	7
Mag	10,000	0,188	18
MP	16,560	0,399	19
NAFZE	1,977	0,524	20
NAFZW	2,435	0,473	10
NAT	2,386	0,349	27
NBS	0,108	1,812	19
PBC	0,780	0,856	12
PP	78,990	-0,340	10
Pyr	0,872	0,672	8
RZ	3,814	0,418	10
SAC	87,220	-0,170	10
SBS	4,959	0,722	27
Sic	22,250	0,123	10
SWP	0,096	1,412	11
Vra	3,336	0,177	133
WA	1,239	0,569	9
WM	99,890	-0,001	106
WTGF	3,861	0,265	20

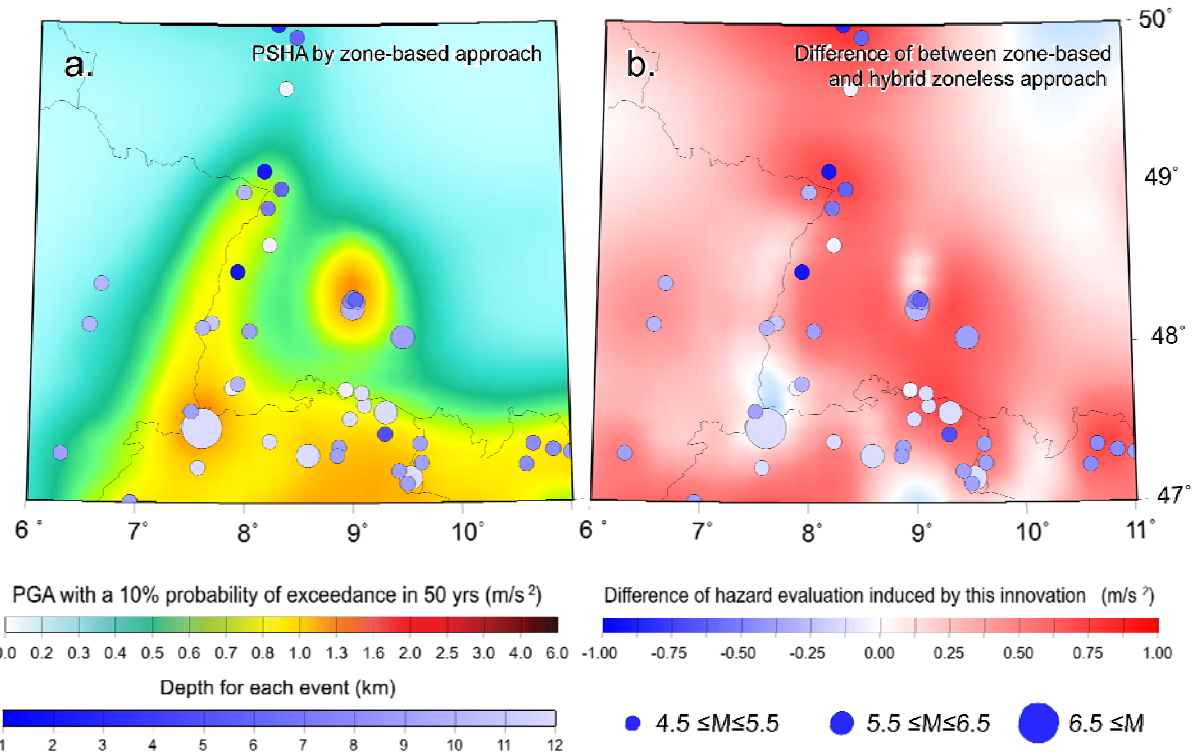


**Figure 7.** (a) The probabilistic ground motion acquired from the zone-based approach by Grünthal *et al.* (2006) and (b) difference with the hybrid zoneless results (Figure 6f).

where  $L$  is the rupture length in km;  $M_w$  is the moment magnitude;  $W$  is the rupture width in km. Ground motion is estimated according to the nearest distance between rupture faults and the target point.

The resulting PGA in the Euro-Med region (Figure 8a) represents the areal distribution of seismicity very well. In comparison with, e.g., the results of GSHAP (Figure 8b), the PGA according to the hybrid zoneless approach show lower values. Such differences are to extent caused due to the different GMPE applied in both projects. Generally, the PGA values in the map according to this study are lower with respect to GSHAP. Previously calculated significant hazardous areas, e.g. in SW Norway, are no more striking.

Due to the required lower magnitude threshold for the application of the used GMPE many small magnitude events with  $M_w < 4.3$  are not used at all in the approach. This leads obviously to an underestimation in the hazard in areas where the maximum magnitudes of observed events are near to or even below this value, since no extrapolation to higher expected, but not observed magnitudes is possible with the method.

The Maghreb (Mag) represents the active boundary between the Eurasian and the African plate. In this zone, a high hazard level with  $\text{PGA} > 2 \text{ m/s}^2$  is evaluated. This can be attributed mainly to high seismicity density along Algerian coastline. Besides, the hybrid approach considers the actual depths of all earthquakes and the applied GMPE predicts high ground motion levels when hypocentral distances are small.

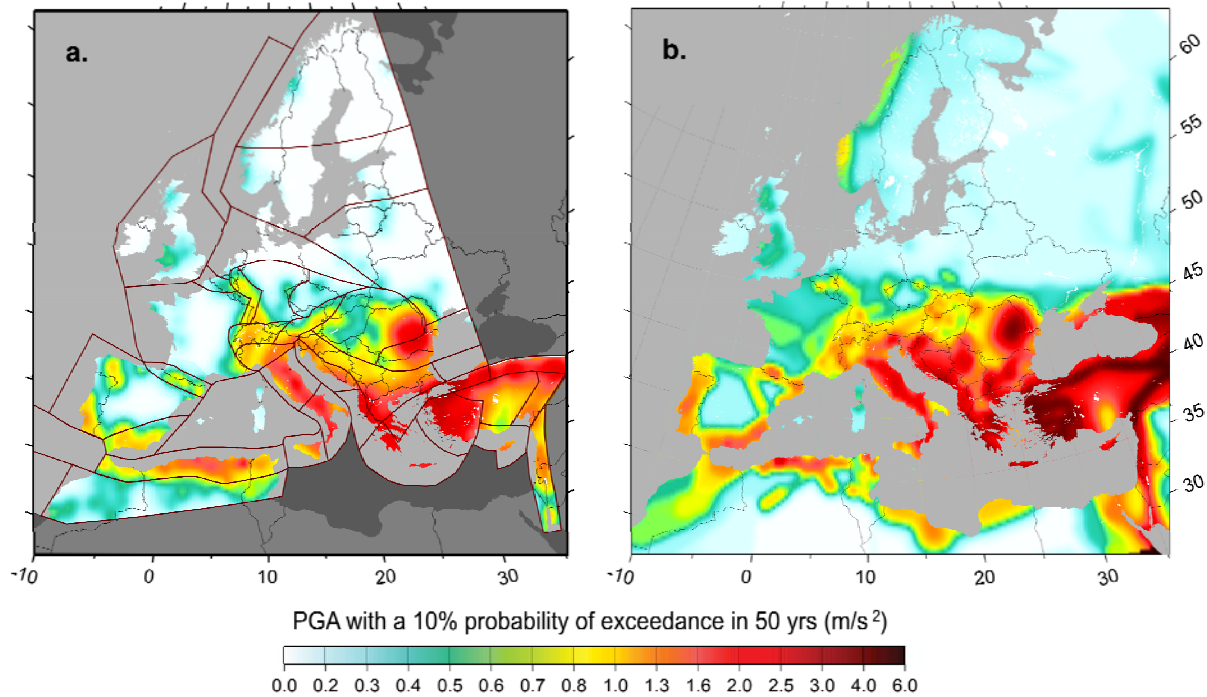


**Figure 8.** The peak ground acceleration (PGA) with a 10% probability of exceedance in 50 years predicted (a) in this study and (b) by the Global Seismic Hazard Assessment Program.

In the Italian peninsula, a high hazard level with peak of 2.6 m/s<sup>2</sup> is calculated along the Apennines (Apn). Our results represent significant lower hazard also in the central and northern parts of the Balkans. Further south, the plate boundary merges into the Aegean subduction zone (ASZ). Here the GMPE by *Atkinson and Boore* (2003) is introduced for the subduction events. A higher hazard with PGA > 2.0 m/s<sup>2</sup> is generated for this zone.

At the southeastern tip of the Pannonian Basin, i.e. in Vrancea region (Vra), with intermediate depth seismicity, we use the GMPE by *Sokolov et al.* (2008). It results in fairly high PGA values and would require additional checking to constrain this result.

SW of the Iberian peninsula the significant historical earthquakes of 1755 ( $M_w = 8.5$ ) or 1969 ( $M_w = 7.8$ ) would require extended sources as well. A significant higher hazard should be expected if this event is treated as extended source with a N-S trending fault orientation as suggested by *Muir-Wood and Mignan* (2009).

## 6. Conclusions

For the traditional zone-based approach (*Cornell*, 1968 and *McGuire*, 1978), several assumptions and information for each seismic source zone are required. Thus, some revisions of model assumptions may be required when significant events take place in a region where events occurred seldom in the past, for ex-

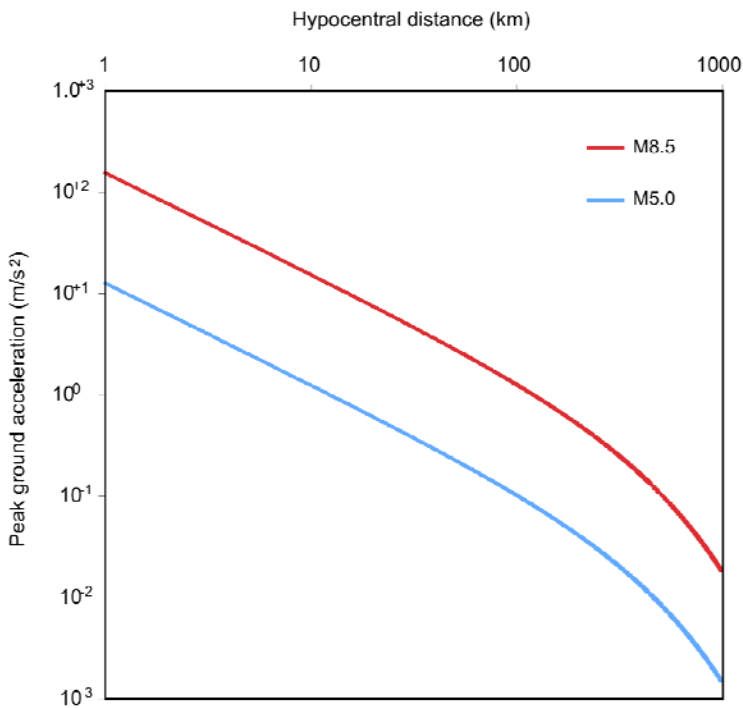


**Figure 9.** The peak ground acceleration (PGA) as a function of hypocentral distance (km) predicted by the prediction equation (GMPE) by Berge-Thierry *et al.* (2003). Red and blue lines represent PGA for earthquakes with magnitude of 8.5 and 5.0, respectively.

ample, the geometry of seismic source zones and/or the distribution of focal depths may need to be revised. Thus, it is difficult to provide new hazard maps automatically without additional adjustments.

For the hybrid zoneless approach we develop in this study, by contrast, the only assumption is the geometry of the large-scale zones controlled by the large-scale geological architecture, which does not require revisions due to spatial and temporal changes of seismicity. Thus, it provides a suitable basis for application to extensive analysis areas and automatically performed PSHA in regular time steps according to the updated earthquake catalogue.

## References

- Atkinson, G.M., Boore, D.M.: Empirical ground-motion relations for subduction-zone earthquakes and their application to Cascadia and other regions. *Bulletin of the Seismological Society of America* **93** (4), 1703-1729, 2003.
- Akkar, S., Bommer, J.J.: Prediction of elastic displacement response spectra in Europe and the Middle East. *Earthquake Engineering and Structural Dynamics* **36** (10), 1275-1301, 2007.
- Akkar, S., Bommer, J.J.: Empirical Equations for the Prediction of PGA, PGV, and Spectral Accelerations in Europe, the Mediterranean Region, and the Middle East. *Seismological Research Letters* **81** (2), 195-206, 2010.

- Ambraseys, N.N., Simpson, K.A., Bommer, J.J.: Prediction of horizontal response spectra in Europe. *Earthquake Engineering and Structural Dynamics* **25** (4), 371-400, 1996.
- Beauval, C., Scotti, O., Bonilla, F.: The role of seismicity models in probabilistic seismic hazard estimation: comparison of a zoning and a smoothing approach. *Geophysical Journal International* **165** (2), 584–595, 2006.
- Berge-Thierry, C., Cotton, F., Scotti, O.: New empirical response spectral attenuation laws for moderate European earthquakes, *Journal of Earthquake Engineering* **7** (2), 193-222, 2003.
- Borcherdt, R.D., 1994. Estimates of site dependent response spectra for design (methodology and justification). *Earthquake Spectra* **10**, 617–654.
- Bungum, H., Lindholm, C.D. and Dahle, A.: Long-period ground-motions for large European earthquakes, 1905–1992, and comparisons with stochastic predictions. *Journal of Seismology* **7** (3), 377– 396, 2003.
- Burkhard, M., Grünthal, G.: Seismic source zone characterization for the seismic hazard assessment project PEGASOS by the Expert Group 2 (EG 1b). *Swiss Journal of Geosciences* **102** (1), 149-188, 2009.
- Cornell, C.A.: Engineering Seismic risk analysis. *Bulletin of the Seismological Society of America* **58** (5), 1583-1606, 1968.
- Drouet, S., Scherbaum, F., Cotton, F., Souriau, A.: Selection and ranking of ground motion models for seismic hazard analysis in the Pyrenees. *Journal of Seismology* **11** (1), 87-100, 2007.
- Frankel, A.: Mapping seismic hazard in the Central and Eastern United States. *Seismological Research Letters* **66** (4), 8-21, 1995.
- Grünthal, G.: The up-dated earthquake catalogue for the German Democratic Republic and adjacent areas - statistical data characteristics and conclusions for hazard assessment. 3rd International Symposium on the Analysis of Seismicity and Seismic Risk (Liblice/Czechoslovakia). *Proceedings Vol. I*, 19-25, 1985.
- Grünthal G, GSHAP Region 3 Working Group: Seismic hazard assessment for central, north and northwest Europe: GSHAP Region 3. *Annali di Geofisica* **42** (6), 999-1011, 1999a.
- Grünthal, G., Bosse, C., Sellami, S., Mayer-Rosa, D., Giardini, D.: Compilation of the GSHAP regional seismic hazard for Europe, Africa and the Middle East. *Annali di Geofisica* **42** (6), 1215-1223, 1999b.
- Grünthal, G., Thieken, A.H., Schwarz, J., Radtke, K., Smolka, A., Merz, B.: Comparative Risk Assessments for the City of Cologne – Storms, Floods, Earthquakes. *Natural Hazards* **38** (1-2), 21-44, 2006.
- Grünthal, G., Wahlström, R.: A harmonized seismicity data base for the Euro-Mediterranean region. In: Oth, A. (ed.): *Cahiers du Centre Européen de Géodynamique et de Séismologie* **28**, Proceedings of the 27th ECGS Workshop "Seismicity Patterns in the Euro-Med Region", Luxembourg, 15-21, 2009.

- Grünthal, G., Wahlström, R., Stromeyer, D.: Harmonization check of  $M_w$  within the central, northern, and northwestern European earthquake catalogue (CENEC). *Journal of Seismology* **13** (4), 613-632, 2009b.
- Grünthal, G., Wahlström, R., Stromeyer, D.: The unified catalogue of earthquakes in central, northern, and northwestern Europe (CENEC) - updated and expanded to the last millennium. *Journal of Seismology* **13** (4), 517-541, 2009a.
- Ivan, I.A., Enescu, B.D., Pantea, A.: Input for seismic hazard assessment using Vrancea source region. *Romanian Journal of Physics* **43**, 619-636, 1998.
- Jiménez, M.-J., Giardini, D., Grünthal, G.: The ESC-SESAME unified hazard model for the European-Mediterranean region. *EMSC/CSEM Newsletter* **19**, 2-4, 2003.
- Mandrescu N., Radulian M.: Macroseismic field of the Romanian intermediate-depth earthquakes, in "Vrancea Earthquakes: Tectonics, Hazard and Risk Mitigation" (eds. F. Wenzel, D. Lungu, O. Novak), Kluwer Academic Publishers, 163-174, 1999.
- Mandrescu, N, Anghel, M, Smalberger, V.: The Vrancea intermediate-depth earthquakes and the peculiarities of the seismic intensity distribution over the Romanian territory. *Studii si Cercetaride Geologie, Geofizica, Gergrafie, GEO-FIZICA* **26**, 51-7, 1988.
- McGuire, R.K.: FORTRAN Computer Program for Seismic Risk. *Open File Report* No 76-67, U.S.G.S., Denver, 1976.
- McGuire, R.K.: FRISK: Computer program for seismic risk analysis using faults as earthquake sources. *Open File Report* No 78-1007, U.S.G.S., Denver, 1978.
- Molina, S., Lindholm, C.D., Bungum, H.: Probabilistic seismic hazard analysis: zoning free versus zoning methodology. *Bulletino di Geofisica Teorica Applicata* **42** (1-2), 19-39, 2001.
- Muir-Wood, R., Mignan, A.: A Phenomenological Reconstruction of the  $Mw9$  November 1st 1755 Earthquake Source. In: Mendes-Victor, L., Sousa Oliveira, C., Azevedo, J., Ribeiro, A. (eds.): The 1755 Lisbon Earthquake: Revisited, *Geotechnical, Geological, and Earthquake Engineering* **7**, Springer, 121-146, 2009.
- Papazachos, B.C., Papaioannou, C.A., Margaris, B.N., Theodulidis, N.P.: Regionalization of seismic hazard in Greece based on seismic sources. *Natural Hazards* **8** (1), 1-18, 1993.
- Papaioannou, C., Papazachos, B.C.: Time-independent and time-dependent seismic hazard in Greece based on seismogenic sources. *Bulletin of the Seismological Society of America* **90** (1): 22-33, 2000.
- Riznichenko, Y.V.: From the activity of earthquake foci to the shakeability of the Earth's surface. *Izv. Acad. Sci. U.S.S.R., Fizika Zemli* **11**, 1-13, 1965.
- Scherbaum, F., Bommer, J. J., Bungum, H., Cotton, F. & Abrahamson, N. A.: Composite ground-motion models and logic trees: methodology, sensitivities, and uncertainties, *Bulletin of the Seismological Society of America* **95** (5), 1575-1593, 2005.

- Sokolov, V., Bonjer, K.-P., Wenzel, F., Grecu, B., Radulian, M.: Ground motion prediction equations for the intermediate depth Vrancea (Romania) earthquakes. *Bulletin of Earthquake Engineering* **6** (3), 367-388, 2008.
- Stucchi, M., Albini, P., Mirto, C., Rebez, A.: Assessing the completeness of Italian historical earthquake data. *Annals of Geophysics* **47** (2/3), 659-673, 2004.
- Suckale, J., Grünthal, G.: A probabilistic seismic hazard model for Vanuatu. *Bulletin of the Seismological Society of America* **99** (4), 2108-2126, 2009.
- Wells, D.L., Coppersmith, K.J.: New empirical relationships among magnitude, rupture length, rupture width, rupture area, and surface displacement. *Bulletin of the Seismological Society of America* **84** (4), 974-1002, 1994.
- Woo, G.: Kernel Estimation Methods for Seismic Hazard Area Source Modeling. *Bulletin of the Seismological Society of America* **86** (2), 353-362, 1996.